The EMBO Journal (2004) 23, 3259–3269 | © 2004 European Molecular Biology Organization | All Rights Reserved 0261-4189/04
www.embojournal.org

THE EMBO JOURNAL

Paraxial protocadherin coordinates cell polarity during convergent extension via Rho A and JNK

Frank Unterseher[1,4], Joerg A Hefele[1,4], Klaudia Giehl[2], Eddy M De Robertis[3], Doris Wedlich[1] and Alexandra Schambony[1,*]

[1]Universität Karlsruhe, Zoologisches Institut II, Karlsruhe, Germany, [2]Universität Ulm, Abteilung Pharmakologie und Toxikologie, Ulm, Germany and [3]Howard Hughes Medical Institute, University of California, Los Angeles, CA, USA

Convergent extension movements occur ubiquitously in animal development. This special type of cell movement is controlled by the Wnt/planar cell polarity (PCP) pathway. Here we show that *Xenopus* paraxial protocadherin (XPAPC) functionally interacts with the Wnt/PCP pathway in the control of convergence and extension (CE) movements in *Xenopus laevis*. XPAPC functions as a signalling molecule that coordinates cell polarity of the involuting mesoderm in mediolateral orientation and thus selectively promotes convergence in CE movements. XPAPC signals through the small GTPases Rho A and Rac 1 and c-jun N-terminal kinase (JNK). Loss of XPAPC function blocks Rho A-mediated JNK activation. Despite common downstream components, XPAPC and Wnt/PCP signalling are not redundant, and the activity of both, XPAPC and PCP signalling, is required to coordinate CE movements.

The EMBO Journal (2004) **23,** 3259–3269. doi:10.1038/sj.emboj.7600332; Published online 5 August 2004
Subject Categories: cell & tissue architecture; development
Keywords: convergent extension; JNK; planar cell polarity; Rho A; XPAPC

Introduction

In vertebrates, coordinated morphogenetic movements shape the dorsal anterior–posterior axis during gastrulation. Convergence and extension (CE), a specific type of cell layer movements, underlie many events in embryonic development like germ band extension in *Drosophila*, elongation of the nematode body axis, and elongation of notochord and somitic mesoderm in vertebrates. The cellular events have been intensely studied in the mesoderm during *Xenopus* gastrulation. All cells polarize along the mediolateral (ML) axis and adopt a bipolar shape. Narrowing and elongation of the tissue is achieved by coordinated radial and ML intercalation thereby coupling convergence and extension (Keller *et al*, 2000; Keller, 2002). In *Xenopus* and zebrafish, CE is controlled by BMP signalling, and the canonical and noncanonical Wnt pathways. We have shown previously that blocking of the canonical Wnt pathway completely inhibits these morphogenetic movements due to reduced Xnr-3 expression (Kuehl *et al*, 2001). The noncanonical Wnt pathway is probably best characterized in *Drosophila*, where it controls planar cell polarity (PCP) in the wing and the ommatidia (Tree *et al*, 2002; Bastock *et al*, 2003; Rawls and Wolff, 2003). A number of downstream components of the PCP pathway, like frizzled (fz), dishevelled (dsh), strabism, and prickle, are highly conserved throughout evolution. In vertebrates, PCP signalling is activated by Wnt-11 and Wnt-5, and controls morphogenetic movements (Heisenberg *et al*, 2000; Darken *et al*, 2002; Park and Moon, 2002; Wallingford and Harland, 2002; Kilian *et al*, 2003; Takeuchi *et al*, 2003; Veeman *et al*, 2003). It has been demonstrated recently that members of the Rho family, Rho A, Rac 1, and cdc 42, act downstream of noncanonical Wnt signalling. These small GTPases regulate different cellular responses such as tissue separation, lamellipodia formation, cytoskeleton rearrangements, cell adhesion, and activation of c-Jun N-terminal kinase (JNK) (Winklbauer *et al*, 2001; Choi and Han, 2002; Yamanaka *et al*, 2002; Habas *et al*, 2003; Penzo-Mendez *et al*, 2003). Modulation of cell adhesion is a central element in convergent extension. The role of integrins and extracellular matrix proteins like fibronectin, Cyr 61, and the glypican knypek for convergent extension and PCP signalling has been emphasized by recent publications (Marsden and DeSimone, 2001, 2003; Topczewski *et al*, 2001; Davidson *et al*, 2002; Latinkic *et al*, 2003). In addition to extracellular cell–matrix adhesion, a role of cell–cell adhesion via cadherins has been implicated (Kuehl *et al*, 1996; Zhong *et al*, 1999; Marsden and DeSimone, 2003).

Paraxial protocadherin (PAPC) is a cell adhesion molecule that has also been shown to promote morphogenetic movements in *Xenopus*. It is expressed first in the Spemann organizer and then in the paraxial mesoderm of the gastrulating embryo (Kim *et al*, 1998) and has been identified as a *LIM 1* target gene in mouse and *Xenopus* recently (Hukriede *et al*, 2003). Interestingly, overexpression of XPAPC mRNA was shown to trigger gastrulation movements in animal cap explants (Kim *et al*, 1998), and in embryos depleted for *LIM 1* in which head structures fail to form (Hukriede *et al*, 2003). Here we report that *Xenopus* paraxial protocadherin (XPAPC) coordinates PCP in cooperation with the Wnt/PCP pathway during gastrulation. Loss-of-function experiments using XPAPC antisense morpholino oligonucleotides (XPAPC-MO) reveal a requirement for convergence, but not for elongation, of the involuting mesoderm. We have characterized the underlying signalling pathways and show that XPAPC exerts its function by activation of JNK via Rho A and simultaneous inactivation of Rac 1.

Results

XPAPC controls convergence in CE movements

We investigated the role of paraxial protocadherin XPAPC during CE movements using a morpholino oligonucleotide (MO) knockdown. We designed two XPAPC-MOs to knock

*Corresponding author. Universität Karlsruhe, Zoologisches Institut II, Kaiserstrasse 12, 76128 Karlsruhe, Germany. Tel.: +49 721 608 4195; Fax: +49 721 608 3992; E-mail: schambony@zi2.uka.de
[4]These authors contributed equally to this work

Received: 14 January 2004; accepted: 22 June 2004; published online: 5 August 2004

down both putative pseudoalleles that each suppressed XPAPC translation *in vitro*, but a complete inhibition was only achieved with a mixture of both. An XPAPC-ORF construct without the 5′UTR was not sensitive to either MO (Supplementary Figure 1). Similar results were obtained *in vivo* (H Steinbeisser, personal communication).

To study CE movements, we prepared Keller open face explants and scored them as described by Kuehl *et al* (2001). In the Keller explant, the tissue has been exposed to all endogenous inducing factors and thus it is considered the best model to study convergent extension movements. The tissue elongates *in vitro* and forms a long protrusion, which represents the involuting marginal zone (IMZ; see also Figure 1). Interestingly, we did not observe any inhibition of Keller explant elongation neither by overexpression of full-length XPAPC nor blocking of XPAPC function with a dominant-negative secreted mutant or XPAPC-MO (Figure 1A). However, upon closer examination, we found that about half of the explants injected with dominant-negative (dn) XPAPC or XPAPC-MO exhibited a significant loss of constriction in the IMZ, while full-length XPAPC and a control MO had no effect on constriction (Figure 1B and C).

The observed failure of explants to constrict is measurable and statistically significant. For quantification, the initial length (L_i), total length ($L_i + \text{IMZ}$), total width (w), and width of the IMZ (c) (Figure 1C) were measured. Elongation ($(L_i + \text{IMZ})/L_i$) and constriction (w/c) of explants were calculated and compared. Wild-type explants ($n = 40$) elongated 2.2 ± 0.3-fold and the IMZ showed a strong and sharp 2.5 ± 0.3-fold constriction at the level of the dorsal blastopore lip. Injection of dnXPAPC mRNA ($n = 14$, elongation 2.2 ± 0.2-fold) or XPAPC-MO ($n = 31$, elongation 2.2 ± 0.2-fold) reduced constriction in the IMZ to only 1.6 ± 0.2- and 1.7 ± 0.2–fold, respectively. The examination of cross-sections showed that the lack of constriction broadens the explant at the expense of thickness. The overall number of cells per section and the number of proliferating cells in the IMZ were unchanged (Supplementary Figure 2).

Although XPAPC loss of function impairs constriction in Keller explants, XPAPC-MO did not cause striking anatomical phenotypes in the developing embryo (data not shown). However, *in situ* hybridizations using chordin and XPAPC itself (mRNA is not degraded after MO injection) as markers for axial and paraxial mesoderm revealed laterally expanded distribution of both axial and paraxial cells from stage 10.5 onwards in XPAPC-MO-injected embryos. In the wild type, a continuous narrowing of the chordin expression domain was observed, until at stage 12 chordin was restricted to the nascent notochord (Figure 2A–C). In XPAPC-MO-injected embryos, we detected a lateral expansion rather than narrowing of chordin staining at stage 11, and at stage 12 the signal is broader and more diffuse, although the notochord is clearly distinguishable (Figure 2D–F). In the paraxial mesoderm, the expression of XPAPC was laterally expanded at all stages (Figure 2K–M) compared to uninjected controls (Figure 2G–J). At stage 12, when XPAPC is excluded from the notochord, we additionally observed a wider and more irregularly shaped gap between the two paraxial expression domains (Figure 2J and M). At stage 20, the expression area of the muscle-specific transcription factor myoD (Figure 2N) was broader on the injected side by $19 \pm 1.3\%$

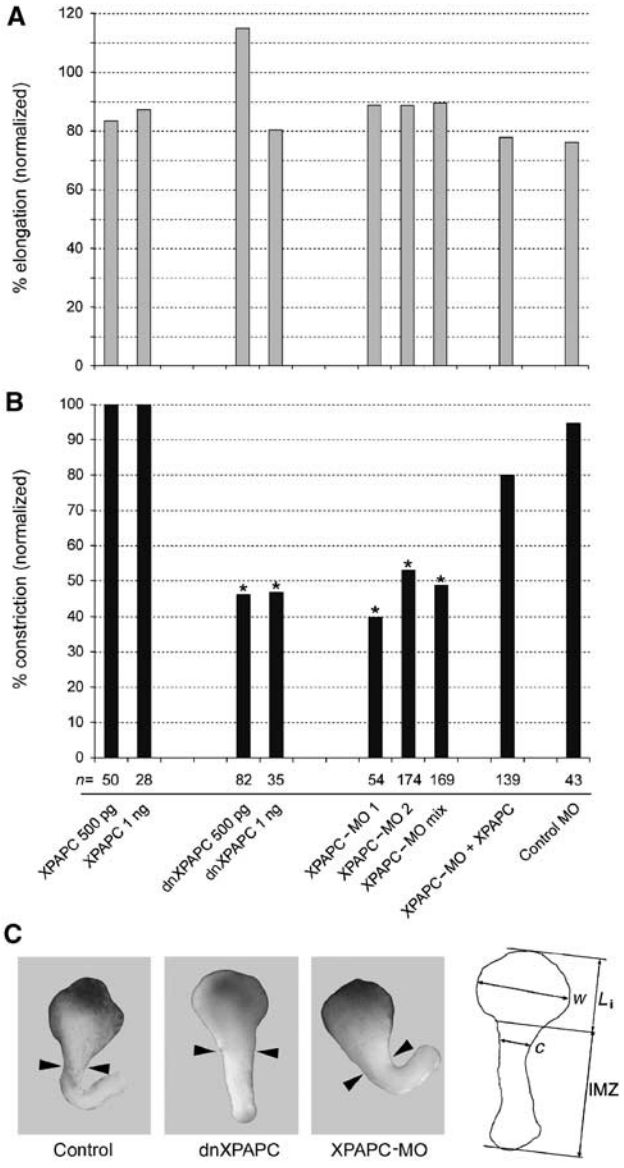

Figure 1 XPAPC loss of function inhibits convergence but not elongation. Explants from embryos injected with full-length XPAPC, dnXPAPC, or two XPAPC-MOs were scored for elongation and constriction. Coinjection of 500 ng of an MO-insensitive XPAPC-ORF construct rescued XPAPC-MO; an unrelated MO (control MO, 100 μM) served as a control. (**A**) The percentage of elongated explants was calculated relative to uninjected controls from the same egg batch. Mean values of at least three experiments are shown. (**B**) The proportion of constricted explants was again normalized to uninjected controls. Asterisks mark values that differ significantly from the control according to Student's *t*-test ($P = 0.99$). (**C**) Images of representative examples of wild-type and dnXPAPC- and XPAPC-MO-injected explants. The drawing illustrates the initial length (L_i) and width (w) and the protruding and constricted (c) IMZ.

($n = 23$). Interestingly, the pan-neural marker gene Sox-2 (Figure 2O) was also expanded laterally by $12 \pm 1.3\%$ ($n = 29$). The effect in neural tissue is probably due to a broader distribution of chordin and other organizer-derived neural inducers.

These results indicate that XPAPC loss of function results in a failure of cells to converge properly. However, convergence and extension are commonly considered as

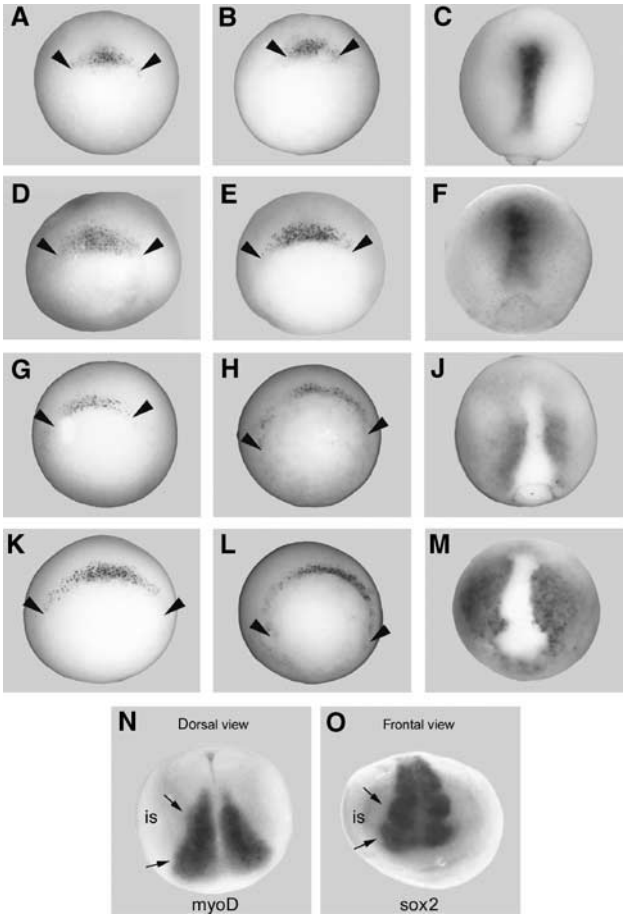

Figure 2 *In situ* hybridization of control and XPAPC-MO-injected explants with chordin (A–F), XPAPC (G–M), myoD, and Sox-2 probes. The expression of chordin becomes restricted in the notochord in wild-type embryos from stage 10.5 (**A**) to 11 (**B**) and 12 (**C**). In XPAPC-MO-injected embryos, broader chordin staining is visible at stage 10.5 (**D**), 11 (**E**), and 12 (**F**). In the wild type, the signal of the XPAPC probe extended laterally from stage 10.5 (**G**) to 11 (**H**). At stage 12, XPAPC is excluded from the axial mesoderm (**J**). The lateral extension of XPAPC staining was enhanced by XPAPC-MO at stage 10.5 (**K**), 11 (**L**), and 12 (**M**). At stage 20, XPAPC-MO injections resulted in broader expression areas of myoD (**N**) in paraxial mesoderm (dorsal view, anterior to the top) and of Sox-2 (**O**) in neural tissue (frontal view, dorsal to the top) on the injected side (is).

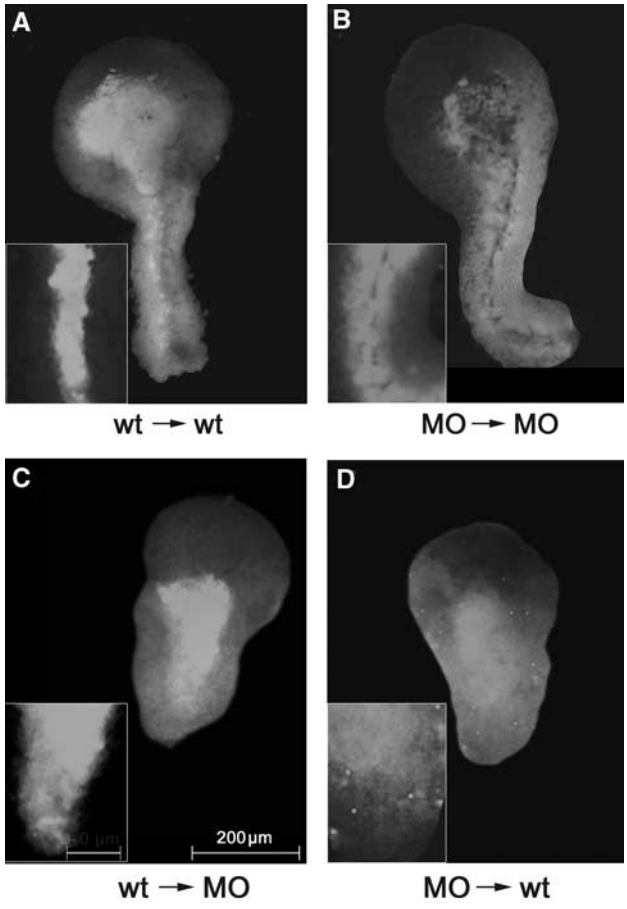

Figure 3 Dorsal marginal zones from fluorescence labelled donor embryos (GFP mRNA in wild-type embryos or DsRed mRNA + XPAPC-MO) were transplanted into Keller explants from unlabelled embryos (wild-type or XPAPC-MO injected). The insets show enlarged fluorescent images. Scale bars apply to all images. (**A**) Transplants from wild-type donors into wild-type hosts (wt→wt). Transplanted, GFP-labelled cells were found in a small stripe along the dorsal midline and formed a sharp border to the host cells (inset). (**B**) Transplants from an XPAPC-MO-injected donor into an XPAPC-MO-injected host (MO→MO). Transplanted cells were found localized in a broad stripe and scattered into unlabelled host tissue (inset). (**C**) Tissue from a wild-type donor in an XPAPC-MO-injected host (wt→MO). The transplant formed a sharp border to the host tissue (inset), but did not converge. (**D**) Transplant from an XPAPC-MO-injected donor in a wild-type host (MO→wt). Cells showed strong scattering behaviour and no constriction. In both cases, where wild-type and MO-injected tissues were mixed, elongation stopped early and the explants never reached full elongation.

coupled processes and furthermore XPAPC is not expressed in the notochord, which undergoes the strongest CE movements. To address this question, we analysed the effect of XPAPC-MO on CE at later stages (see also Supplementary Figure 3). When explants were cut at stage 12.5 and cultured until stages 22–23, both wild-type and XPAPC-MO-injected explants elongated and differentiated into notochord and somites (Supplementary Figure 3A and B). We measured the width of the notochord and the lateral extension of somites in these explants and in sections immunostained for notochord and somitic mesoderm. The notochord of XPAPC-MO-injected embryos was 12% broader ($83 \pm 12\,\mu m$, $n = 16$) than in wild-type embryos ($74 \pm 9\,\mu m$, $n = 12$). The expansion of the notochord, which does not express XPAPC, probably originates from the earlier disorder that is seen in the laterally widened chordin expression (Figure 2). A more pronounced effect was detected in the somitic mesoderm, which extended laterally 27% more in XPAPC-depleted embryos ($138 \pm 27\,\mu m$, $n = 16$) than in controls ($109 \pm 22\,\mu m$, $n = 12$). Although the majority of cells performed the characteristic 90° rotation in the somite, the cells were oriented irregularly and seemed to be loosely packed (Supplementary Figure 3H–L). In contrast, all wild-type cells showed an orientation parallel to the notochord and were tightly stacked. To analyse whether XPAPC-MO inhibits CE only in the prospective somitic mesoderm, we dissected the notochord, and cultured notochord and dorsolateral marginal zone (DLMZ) explants separately. As described by Wilson *et al* (1989), the isolated DLMZ explants elongated without notochord. However, we did not observe any inhibition by XPAPC-MO or a control MO of the elongation of isolated

DLMZs (Supplementary Figure 3A–G). These results show that XPAPC loss of function affects the ML extension, but does not block elongation in the somitic mesoderm.

To better understand the cell behaviour caused by XPAPC-MO, we performed transplantation experiments. A wild-type dorsal marginal zone transplanted into a wild-type Keller explant underwent normal convergent extension. All labelled IMZ cells were localized in a small stripe near the dorsal midline (Figure 3A). When cells were transferred from an XPAPC-MO-injected donor to an XPAPC-MO host, as in nontransplanted explants, normal elongation but inhibition of constriction was observed. The transplanted cells formed a broad stripe and were also found scattered outside the main localization domain (Figure 3B). In transplantations from a wild-type donor to an XPAPC-MO-injected host, the transplanted cells adhered together as in wild type, but did not show constriction (Figure 3C). Cells transplanted from an XPAPC-MO-injected donor to a wild-type host scattered all over the explant (Figure 3D). These results indicate that scattering of cells is caused by XPAPC-MO cell-autonomously. Inhibition of convergence on the other hand is not a cell-autonomous effect. Together, these findings explain the lateral expansion of marker gene expression shown in Figure 2. Interestingly, in both types of mixed transplantation, explants showed neither constriction nor full elongation. When cells lacking XPAPC intermingle with wild-type cells, this could impair the ability to coordinate with neighbouring cells stronger than in a fully XPAPC-depleted tissue and lead to inhibition of CE.

XPAPC loss of function disrupts coordination of cell polarity

During early convergent extension, the mesodermal cells adopt a bipolar shape with the long axis oriented parallel to the ML axis of the embryo and intercalate between each other.

Since our results indicated an inhibition of convergence by XPAPC-MO, we next analysed the polarization and migration behaviour of membrane-tethered GFP (mGFP)-labelled mesodermal cells in the vegetal alignment zone (VAZ) from stage 10.5 onwards. In explants from wild-type embryos, the cells showed the typical elongation and coordinated polarization along the ML axis. In an average of three movies, 86% of cells were oriented within a $\pm 20^\circ$ arc perpendicular to the anterior–posterior axis. Figure 4A and B shows a representative image and a schematic illustration of cell polarity. The cells moved almost exclusively towards the dorsal midline, as illustrated by plotting the migration paths (Figure 4E) and calculating the total and net dorsal speed according to Marlow *et al* (2002) (Figure 4G). Movements appear as a concerted action of all cells, which indicates coordination of cells throughout the dorsal mesodermal layer (see also Supplementary Figure 4). XPAPC-MO injections disrupted the coordination of cell polarity. Although most cells still acquired a bipolar shape, only 39% of cells were ML oriented (Figure 4C and D). The overall polarization was randomized and cells changed their polarity frequently. We observed up to 15 reorientations within 2 h, resulting in a slower, multidirectional migration (Figure 4F and G and Supplementary Figure 5). Similar cell behaviour was seen in dnXPAPC-injected cells (data not shown).

We also investigated the cell behaviour of wild-type and XPAPC-injected explants at later stages. At stage 13+, wild-type cells were elongated (length to width ratio (LWR) 2.0 ± 0.3) and oriented perpendicular ($\pm 18^\circ$ arc) to the notochord and migrated dorsally. The observed total speed between stages 13 and 18 was 32 μm/h and the net dorsal speed was 29 μm/h. XPAPC-MO did not affect cell elongation (LWR 1.8 ± 0.4), but randomized the directions of cell orientation and migration like in early gastrula. We measured a net dorsal speed of 13 μm/h and a total speed of 32 μm/h between stages 13 and 18 (Supplementary Figure 6). These results illustrate that XPAPC loss of function disrupted the coordinated polarity and migration in the mesoderm. We conclude from the results that the XPAPC cell adhesion molecule has profound effects in the coordination of bipolar cells along the ML axis required for CE movements. This is further supported by the subcellular localization of XPAPC, which was monitored using an XPAPC-GFP fusion construct. XPAPC-GFP was detected at the cell membrane and in Golgi vesicles. However, XPAPC-GFP was not distributed ubiquitously over the cell membrane like β1-integrin (Figure 5B and C) or classical cadherins (data not shown), but exhibited a biased localization at medial and lateral cell contacts (Figure 5A, C and D). This asymmetric distribution strongly supports a role of XPAPC in the coordination of cell polarity and CE movements.

XPAPC acts in cooperation with the Wnt/PCP pathway

The defects of coordinated cellular polarity are strikingly similar to defects in PCP pathway components observed in *Drosophila* (Axelrod *et al*, 1998; Tree *et al*, 2002). In *Xenopus*, XWnt-11/Fz 7 signalling has been shown to activate a non-canonical Wnt pathway. Fz 7 induces G-protein-mediated activation of PKC and in addition signals via dishevelled. Inhibition of Wnt/PCP signalling by an Fz 7-MO knockdown had a similar phenotype to XPAPC loss of function. Like XPAPC-MO, Fz 7-MO selectively inhibited constriction without affecting elongation of Keller explants (Figure 6). In contrast to XPAPC (see Figure 1), overexpression of full-length Fz 7 strongly inhibited explant elongation, but did not affect constriction. Activation of PKC, a known downstream component of Fz 7, with PMA only partially rescued Fz 7-MO while dshΔDIX mRNA, which activates only PCP signalling (Wharton, 2003), fully restored constriction but also inhibited elongation of Keller explants. We note that full-length XPAPC could not restore full convergence, nor did coinjections of Fz 7 rescue XPAPC-MO. Rather, the inhibitory effect was enhanced and furthermore a strong decrease in elongation was induced (Figure 6). Activation of PKC with PMA had a similar effect, indicating that XPAPC is not part of the PKC pathway. The coinjection of XPAPC-MO and dshΔDIX mRNA was lethal.

Taken together, these experiments demonstrate that XPAPC and Fz 7 both control cell convergence in Keller explants. However, XPAPC is not rescued by Fz 7 or its downstream effectors, indicating that XPAPC and Fz 7 cannot substitute for each other, but rather appear to act together in the coordination of cellular polarity.

XPAPC controls convergence by RhoA-mediated JNK activation

The small GTPases Rho A, Rac 1 and cdc 42 and the kinase JNK have been identified as downstream effectors of the Wnt/PCP pathway (Sheldahl *et al*, 2003). We therefore

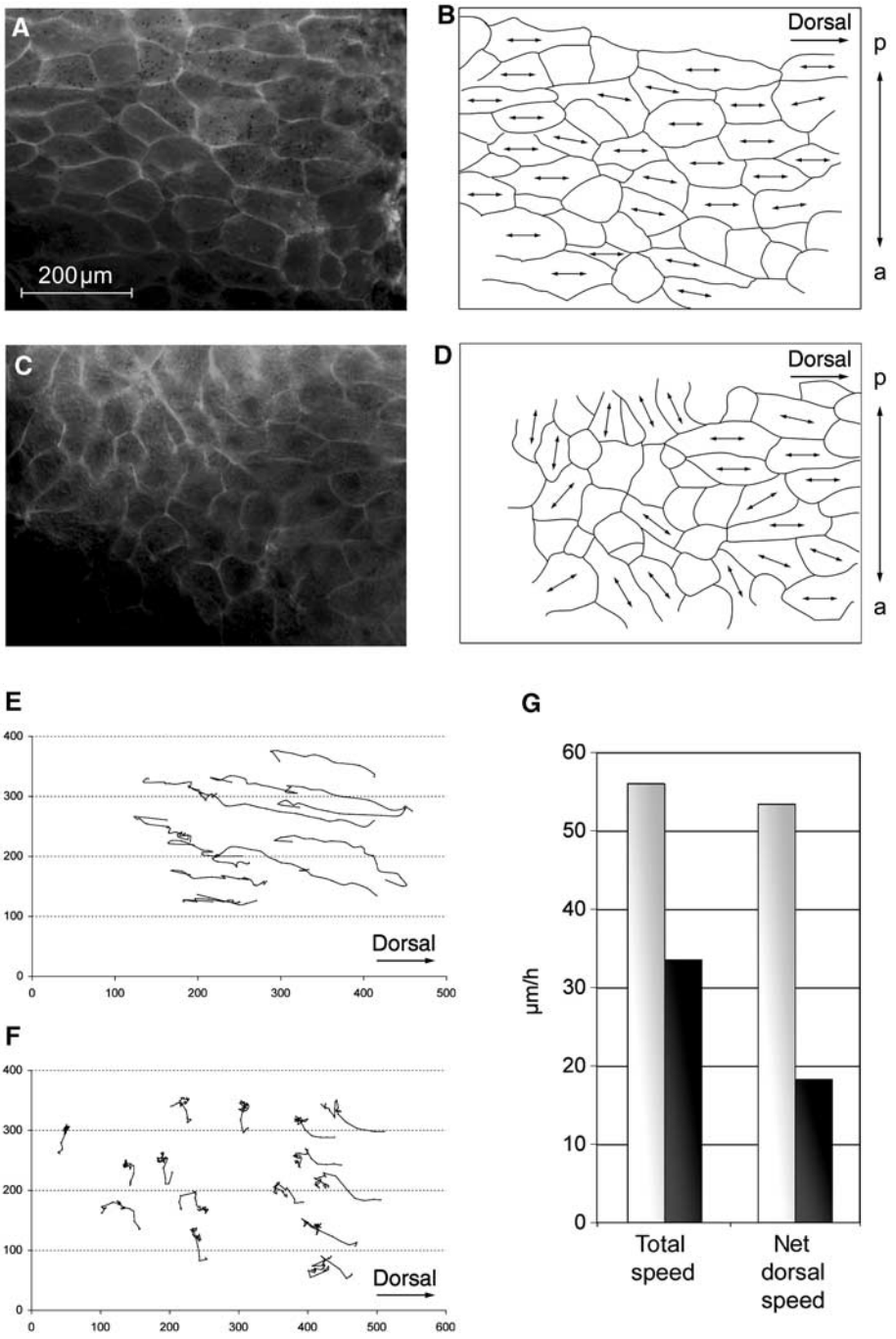

Figure 4 Time-lapse movies were recorded to evaluate cellular behaviour using mGFP to visualize cell membranes. A single image from each movie is shown together with a drawing of the outline of cells. The arrows indicate the long axis of bipolar cells. The complete time-lapse movies are available as supplementary figures. (**A, B**) In wild-type explants, all cells of the involuting mesoderm showed a bipolar form with polarization along the ML axis. (**C, D**) XPAPC-MO-injected explants showed small groups of cells with identical polarization axis, but the overall tissue polarity was randomized and some cells failed to reach the typical bipolar shape. Cells in wild-type (**E**) explants showed dorsally directed migration paths with little or no change of direction. In contrast, in XPAPC-MO-injected (**F**) explants, only 39% of cells showed dorsal migration and all cells often changed direction. The calculated total and net dorsal speeds (**G**) of wild-type (grey bars) and XPAPC-depleted (black bars) explants further confirmed these observations.

investigated whether XPAPC influences the activation of endogenous small GTPases or JNK, and whether these molecules are able to rescue XPAPC loss of function. Pull-down assays for endogenous GTP-bound small GTPases demonstrated that XPAPC overexpression activates Rho A and inhibits Rac 1. Consistently, XPAPC-MO injection blocked Rho A and stimulated Rac 1 (Figure 7A). The activation state of cdc 42 was not changed either by XPAPC overexpression or XPAPC-MO. In addition, we have identified the kinase JNK as a target of XPAPC signalling. As shown in Figure 7A, overexpression of XPAPC mRNA stimulated, and XPAPC-MO injection blocked, endogenous JNK activation. To confirm these results in rescue experiments, we coinjected XPAPC-MO with constitutively active (ca) Rho A or a constitutively active

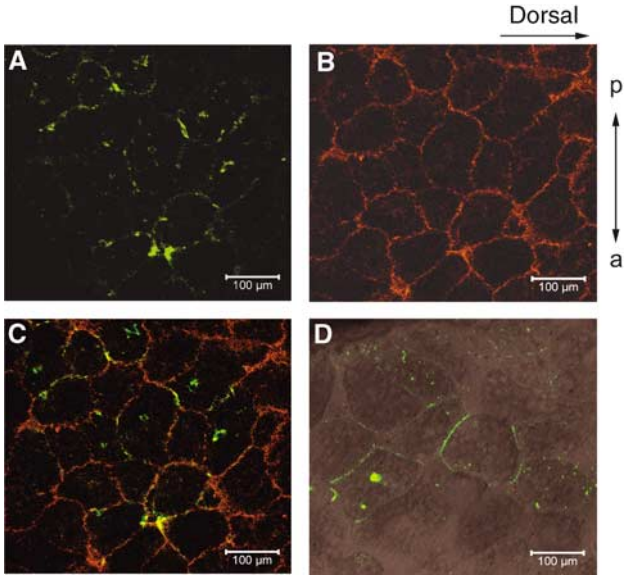

Figure 5 Subcellular localization of XPAPC monitored by an XPAPC-GFP fusion protein. In fixed explants counterstained for β-1-integrin, XPAPC was found localized preferentially to the medial and lateral ends of bipolar cells (**A, C**), while the β-1-integrin (**B**) showed a uniform distribution all over the cell membrane. The biased localization of XPAPC was also seen in live imaging of XPAPC-GFP-injected explants (**D**).

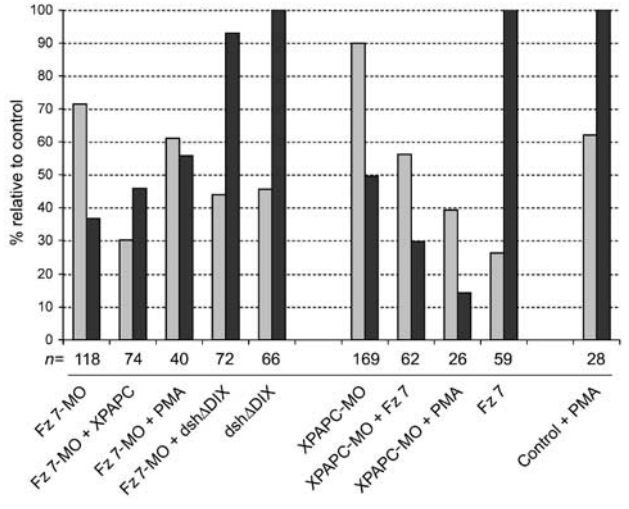

Figure 6 Fz 7-MO phenocopies XPAPC-MO, but neither can substitute for the other. Grey columns represent mean values of fully elongated explants from at least three experiments normalized to uninjected controls of the same egg batch. Black columns show the proportion of fully constricted explants. The explants were excised from embryos injected with Fz 7-MO (500 µM) or XPAPC-MO (100 µM). For rescue experiments, dshΔDIX (500 ng), full-length XPAPC (500 ng), or full-length Fz 7 (500 ng) was coinjected with the MOs. PKC activation was induced by adding 200 nM PMA to the culture medium.

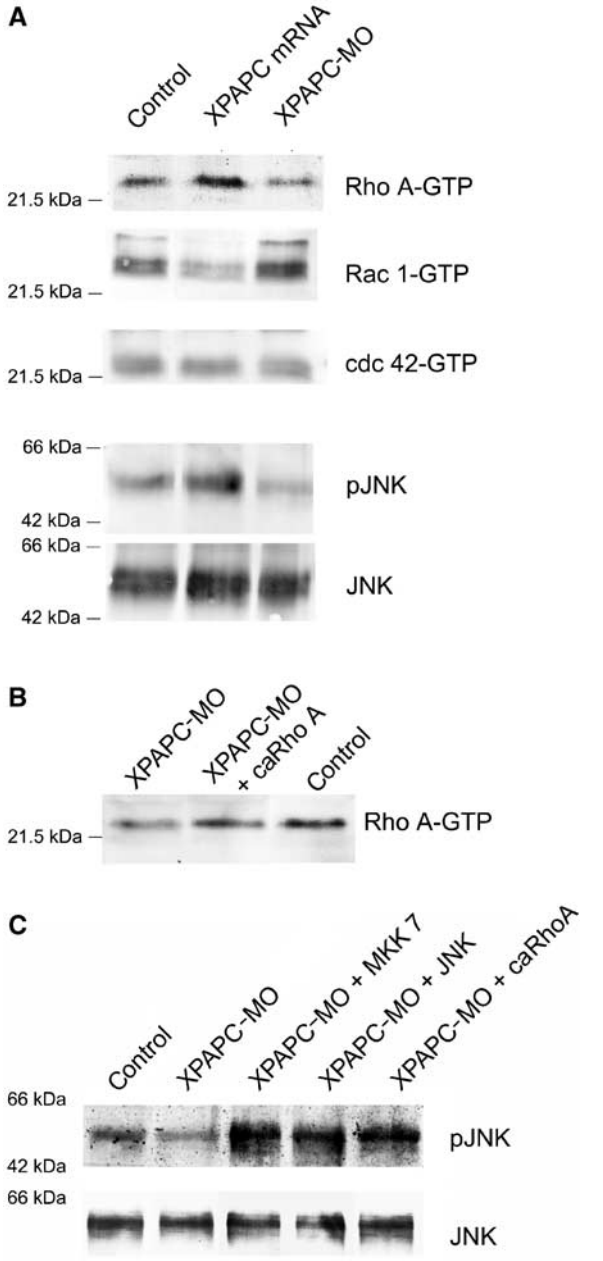

Figure 7 XPAPC regulates Rho A, Rac 1, and JNK. (**A**) The GTP forms of the small GTPases Rho A, Rac 1, and cdc 42 were pulled down from embryo lysates with GST-RBD (Rho-binding domain from Rhotekin) and GST-PAK and normalized to the total protein input. The small GTPases were detected using monoclonal antibodies. XPAPC mRNA activates Rho A and inhibits Rac 1, and does not influence cdc 42 activation. In XPAPC-MO injections, Rho A-GTP is decreased and Rac 1-GTP increased. Active JNK was detected by an antibody selective for the phosphorylated active form. XPAPC overexpression activates JNK, while XPAPC-MO inhibits activation. The loading control below shows the total input of JNK using a polyclonal antibody. (**B**) Coinjection of XPAPC-MO with 5 pg of caRho A plasmid DNA restored the level of Rho A-GTP to control levels. (**C**) Coinjection of XPAPC-MO with either 25 pg caMKK 7 plasmid DNA, 500 pg JNK RNA, or 5 pg caRho A activated JNK above control levels.

mutant of the JNK-activating kinase MKK 7. These constitutively active mutants are very potent and interfere with early development and were therefore injected as plasmid DNA. The presence of active Rho A at the onset of gastrulation was confirmed by a Rho A pull-down assay, which showed that the level of Rho A-GTP was restored to control levels in DNA-injected embryos (Figure 7B). We next analysed the level of active JNK in embryos coinjected with XPAPC-MO and caRho A, caMKK 7 or wild-type JNK. Figure 7C shows that the inhibition of JNK activation by XPAPC-MO was not only

overcome but also enhanced above control levels by coinjection of caMKK 7 as expected. A comparable activation has been achieved by coinjection of wild-type JNK. Remarkably, injection of XPAPC-MO together with caRho A alone was sufficient to reactivate JNK to a similar extent as caMKK 7 or JNK. We conclude from these results that Rho A acts upstream of JNK in XPAPC signalling and is sufficient to mediate JNK activation.

Figure 8A summarizes the effect on Keller explant elongation and constriction. In agreement with the biochemical data, caRho A rescued constriction when coinjected with XPAPC-MO. dnRho A consistently enhanced the inhibition of constriction and also inhibited elongation of the explants. Neither coinjections of caRac 1 nor dnRac 1 restored constriction, but caused a significant reduction in elongation. caMKK 7 only partially rescued XPAPC-MO, but wild-type JNK rescued constriction of Keller explants when coinjected with XPAPC-MO. In addition, we observed a synergistic effect of JNK and caRho A indicating a cooperative action of Rho A and JNK downstream of XPAPC. Control injection of the constructs used in these rescue experiments show that dnRho A and caRac 1, consistent with the biochemical data, blocked both elongation and constriction in a dose-dependent manner. dnRac 1 selectively acted on elongation. Similarly, caMKK 7 induced only weak inhibition of constriction but blocked elongation at higher doses, while caRho A and JNK had only weak effects (Figure 8B).

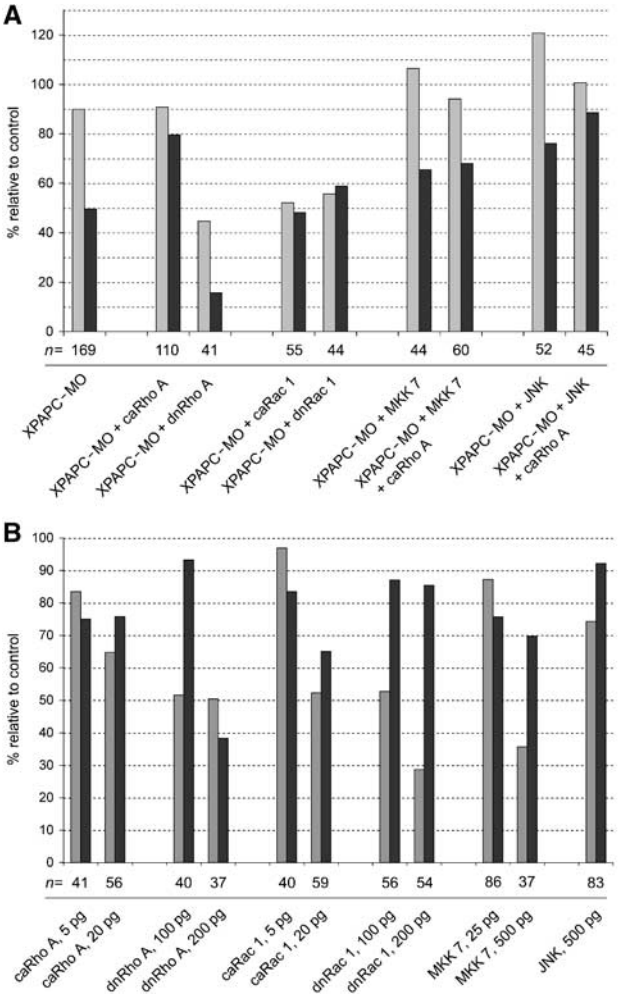

Figure 8 Constitutively active Rho A and JNK rescued constriction in Keller explants from XPAPC-MO-injected embryos. The columns represent mean percentages of fully elongated explants from at least three experiments normalized to uninjected controls of the same egg batch. Grey columns show elongation and black columns show convergence. (**A**) Coinjection of XPAPC-MO with 5 pg caRho A, 100 pg dnRho A, 5 pg caRac 1, 100 pg dnRac 1, 25 pg caMKK 7, 25 pg caMKK 7 + 2.5 pg caRho A, 500 pg JNK, and 500 pg JNK + 2.5 pg caRho A. Constriction was rescued by caRho A and JNK. The best rescue was obtained by coinjection of XPAPC-MO with both caRho A and JNK. (**B**) Explants from embryos injected with caRho A, dnRho A, caRac 1, dnRac 1, caMKK 7, and JNK. All constructs were injected in the concentration used for coinjections (panel A) and an elevated concentration as indicated.

Discussion

Knockdown of XPAPC with antisense MOs has shown that XPAPC coordinates the orientation of bipolar cells along the ML axis. Loss of function results in broadening of the paraxial and axial mesoderm and failure of constriction in Keller explants. Constriction and elongation are the results of CE movements, which in *Xenopus* are considered inseparable. Despite their failure to constrict/converge, XPAPC-depleted Keller explants elongated normally, which might suggest an uncoupling of convergence from extension movements. In zebrafish, the Rho A-dependent kinase (ROK) has been described to influence only convergence (Marlow *et al*, 2002), giving further evidence to the surprising realization that these two processes might not be inextricably connected as previously thought. We presented evidence that XPAPC is capable of activating an intracellular signalling cascade and that it acts through the small GTPases Rho A and Rac 1 and the kinase JNK. We have shown that XPAPC has an inhibitory effect on Rac 1 and does not affect cdc 42. However, inhibition of Rac 1 activation alone seems to be a side effect, as coinjection of dnRac 1 with XPAPC-MO is not sufficient to restore convergence. We identified Rho A and JNK as the downstream effectors of XPAPC that promote convergence and showed that Rho A is sufficient to activate JNK. Thus, XPAPC exerts its function in the coordination of cell polarity via Rho A and through Rho A activates JNK (Figure 9).

Paraxial protocadherin and gastrulation movements

XPAPC was proposed to be part of the structural machinery that converts Spemann organizer regulatory signals into morphogenetic movements on the basis of overexpression experiments (Kim *et al*, 1998). Although the knockout of mouse PAPC did not cause gastrulation phenotypes (Yamamoto *et al*, 2000), its importance in *Xenopus* gastrulation has been highlighted by a recent genome-wide macroarray screen. When the genes that are most strongly activated by the Wnt/β-catenin and the Nodal/TGFβ pathways at gastrula were examined, the strongest transcriptional activation was found for *chordin*, *Xnr-3*, and *XPAPC*, in that order (Wessely *et al*, 2004). Thus, XPAPC is one of the genes most strongly expressed in response to Spemann organizer signals. Although the evidence indicated that XPAPC could function in CE, the molecular mechanisms involved remained unknown. In a previous study, expression of dnXPAPC inhibited elongation of animal caps treated with high levels of activin completely (Kim *et al*, 1998). In Keller

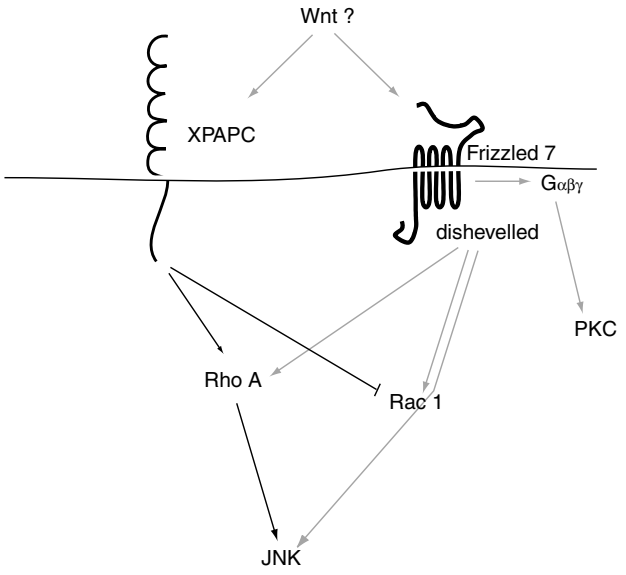

Figure 9 Model of the XPAPC signalling pathway. XPAPC stimulates Rho A, and JNK is activated via Rho A. In parallel, XPAPC inhibits Rac 1. Rho A and JNK activation is essential to control convergence, while inhibition of Rac 1 alone is not sufficient to mediate XPAPC function.

explants, however, this did not block extension. While full-length XPAPC had no significant effect, the dominant-negative construct affected constriction but not elongation of explants (Figure 1). The diverging results in animal caps versus Keller explants could be explained by the different nature of the assay system. In the animal cap assay, mesoderm is induced by members of the TGFβ family, for example, activin or BVg1. However, according to current models, induction and dorsal specification of mesoderm requires not only TGFβ signalling but also β-catenin and other factors present in the dorsal marginal zone (Agius *et al*, 2000). In Keller explants, mesoderm induction and formation of the organizer have already taken place. In this respect, Keller explants differ greatly from the animal cap system. Therefore, it is understandable that these two assay systems might yield different results. In the embryo, no obvious phenotype is induced by XPAPC depletion, but *in situ* hybridizations revealed that both axial mesoderm and paraxial mesoderm are expanded laterally.

The observed broadening of the IMZ cannot be accounted for by an increased number of cells, but rather by a corresponding decrease in thickness. As no inhibition of elongation is observed, this would be contradictory to the common opinion that convergence and extension are coupled. The notochord does not express XPAPC from late gastrula onwards and its cells exhibit the strongest CE movements. Therefore, the notochord might compensate for the inhibition of XPAPC function in the somitic mesoderm and drive elongation of the anterior posterior axis. However, isolated somitic mesoderm of XPAPC-MO-injected embryos showed normal elongation, contradicting this interpretation. Nevertheless, the somitic mesoderm appears disorganized and, although somites are formed, the cells are irregularly and loosely aligned. Taken together, these results indicate an impaired convergence of cells towards the dorsal midline, which is further supported by the striking behaviour of XPAPC-deficient cells. These cells do not converge, but rather tend to scatter laterally, which could be partially due to altered adhesion properties of these cells that facilitate migration. However, if the effects were solely caused by reduced cell adhesion, XPAPC-MO-injected explants would not be expected to elongate. In addition, dissociation of the cells and disintegration of the tissue might be seen, which was not the case. Therefore, XPAPC functions beyond cell adhesion must be assumed.

We have shown that XPAPC-MO affects the coordination of cell polarity. XPAPC is expressed throughout the VAZ before the notochord is formed. XPAPC-depleted cells are still able to elongate and exhibit a bipolar shape, but show arbitrary orientation, as they do not align along the ML axis and migrate in random directions. At later stages, we observed in the somitic mesoderm that wild-type cells elongated, aligned perpendicular to the notochord, and moved towards the notochord. XPAPC-MO impaired the coordinated alignment of cells and randomized migration as in the VAZ at early gastrula. Thus, XPAPC function is required for CE throughout the anterior–posterior elongation process of the embryo. XPAPC loss of function disrupts the ML orientation of cells, while anterior–posterior extension of mesodermal tissue is not affected. The original definition (Shih and Keller, 1992; Keller *et al*, 2000) that convergence means ML orientation and intercalation without a directional preference is not questioned. Instead, the role of XPAPC is seen to confer ML information to a cell layer in coordinating cells via asymmetric subcellular localization at the medial and lateral cell membranes. Thereby, XPAPC selectively controls convergence and thus uncouples to some extent convergence from extension.

Downstream of XPAPC signalling: Rho A, Rac 1, and JNK

The changes in cellular behaviour induced by interfering with XPAPC function point to a connection with the PCP signalling pathway. We have demonstrated that inhibition of the Wnt/PCP signalling pathway by an Fz 7-MO knockdown (Winklbauer *et al*, 2001) phenocopies XPAPC loss of function. Keller explants were so far evaluated only for elongation and we are the first to describe a broader IMZ phenotype. As Fz 7-MO, like XPAPC-MO, does not affect elongation, it is not surprising that no effect on CE was described earlier. Interestingly, we were not able to rescue Fz 7-MO with XPAPC or vice versa. These results point towards a functional connection between Wnt/PCP signalling and XPAPC signalling, but also indicate that these two pathways are not redundant. The Wnt/PCP pathway and XPAPC signalling, however, are not independent. We have identified Rho A, Rac 1, and JNK as XPAPC targets and also these molecules are part of the Wnt/PCP pathway. Recently published data show that XPAPC and Rho A act downstream of LIM 1 in the control of morphogenetic movements in *Xenopus* (Hukriede *et al*, 2003). Our results not only support this but also identify Rho A as a component of an XPAPC-activated signalling cascade. In the Wnt/PCP pathway, dishevelled activates both Rho A and Rac 1 and via Rac 1 also JNK (Habas *et al*, 2003). In contrast, XPAPC inhibits Rac 1 and acts through Rho A to activate JNK (Figure 9). This is in agreement with previously published data that JNK is an essential effector molecule in convergent extension (Yamanaka *et al*, 2002). Recent studies

show that JNK phosphorylates paxillin, a component of the focal adhesion complex and promotes cell migration on an extracellular matrix (Huang *et al*, 2003). It is becoming apparent that not only cell–cell adhesion but also cell–matrix adhesion is required during convergent extension (Davidson *et al*, 2002), and that integrin function and adhesion to fibronectin influence cadherin-mediated cell adhesion (Marsden and DeSimone, 2003). This study demonstrates that XPAPC, a cell–cell adhesion molecule located preferentially at medial and lateral cell membranes in the direction of convergence, transduces signals to the machinery of small GTPases and JNK that controls cell migration and extracellular matrix adhesion. Rho A and Rac 1 play distinct roles in cell migration and convergent extension. Rho A promotes cell motility, while Rac 1 is reported to enhance cell adhesion (Kaibuchi *et al*, 1999). During convergent extension, the activity of both Rho A and Rac 1 is required for polarization and protrusive activity, but additionally Rho A regulates cell shape and Rac 1 controls filopodia formation in intercalating cells (Tahinci and Symes, 2003). In agreement with this, XPAPC loss of function causes random polarization and migration direction (Figure 4), resembling the lack of Rho A activity.

In conclusion, loss-of-function studies indicate that convergence of the IMZ towards the dorsal midline and of the somitic mesoderm towards the notochord require XPAPC. The XPAPC protein accumulates in medial and lateral cell surfaces pointing towards the dorsal midline. This polarized localization suggests an important role for these cell surfaces in convergence movements. XPAPC is not only a cell adhesion molecule but is also able to signal through the Wnt/PCP pathway via Rho A and JNK to coordinate and synchronize cell movements within the mesodermal germ layer. We also show that the Wnt receptor Fz 7 has similar phenotypes to those of PAPC signalling and that Fz 7 and XPAPC are not redundant. Our results point towards a combined action of Fz 7 and XPAPC. This interpretation is supported by the demonstration of a physical interaction between the extracellular domains of XPAPC and Fz 7 (H Steinbeisser, personal communication). Future studies on the XPAPC protocadherin will be directed towards understanding how Wnt/PCP and protocadherin signalling are integrated to execute complex behaviours of germ layers during morphogenesis.

Materials and methods

Frog handling and microinjections

Embryos were obtained by *in vitro* fertilization, cultured and injected as described previously (Geis *et al*, 1998). Staging followed the normal table of Nieuwkoop and Faber (1975). RNA for microinjections was prepared using the mMessage mMachine Kit (Ambion, Austin, TX) as described (Geis *et al*, 1998). The injection amount varied depending on the construct: XPAPC and XPAPC mutants 500 pg or 1 ng (Kim *et al*, 1998), dsh mutants 500 pg (Miller *et al*, 1999), JNK 500 pg (Nishitoh *et al*, 1998), mGFP 100 pg, and mDsRed2 100 pg. In some cases, plasmid DNA, rather than mRNA, was injected to avoid early effects: constitutive-active (ca) Rho A (V14) 2.5–10 pg, dnRho A (N19), caRac 1 (V12), dnRac 1 (N17), and caMKK 7 25–50 pg (Yamanaka *et al*, 2002). For the XPAPC-GFP constructs, GFP has been fused to the carboxy-terminus of XPAPC by PCR and cloned into the pCS2+ vector. XPAPC-MOs were designed to bind to the 5′UTR 60–80 nucleotides upstream of the AUG codon of both XPAPC pseudoalleles. XPAPC-MO 1, 5′-cctagaaacagtgtggcaatgtgaa-3′, matches to XPAPC (AF042192), and XPAPC-MO 2, 5′-cttgcctagaaagagtgctgctgtg-3′, matches to *Xenopus* EST BU911425. XPAPC-MOs were injected as 100 μM solution or as a mixture of 50 μM of each MO. The standard control MO provided by Gene Tools, 5′-cctcttacctcagttacaatttata-3′ (all MOs: GeneTools, Philomath, OR), served as a negative control. Fz 7-MO (Winklbauer *et al*, 2001) was used in a 500 μM concentration.

In situ hybridization

Whole-mount *in situ* hybridizations were carried out using the digoxygenin/alkaline phosphatase detection system (Roche Molecular Biochemicals, Mannheim, Germany) as described (Hollemann *et al*, 1999). The myoD probe was kindly provided by Ralph Rupp.

Keller explants and time-lapse microscopy

Keller open face explants (Keller *et al*, 1992; Shih and Keller, 1992) were prepared at stage 10.5 and cultured in 1 × MBS (10 mM HEPES pH 7.4, 88 mM NaCl, 1 mM KCl, 2.4 mM Na_2CO_3, 0.82 mM $MgSO_4$, 0.33 mM $Ca(NO_3)_2$, 0.41 mM $CaCl_2$) till stages 13–14. Explants were classified in three categories as described previously (Kuehl *et al*, 2001). Elongation was normalized to uninjected controls of the same egg batch. Constriction expresses the normalized proportion of elongated explants that show normal constriction. To analyse later effects, explants were cut between stages 12.5 and 13 and the notochord was excised to obtain isolated DLMZ explants (Wilson *et al*, 1989). Transplantations were carried out at stage 10.5. Donor embryos were labelled with mGFP or DsRed containing a palmitoylation signal (Kim *et al*, 1998). An area of approximately 0.1 mm × 0.1 mm was cut above the dorsal blastopore lip and transferred into the host explant. For time-lapse microscopy, mGFP-labelled explants were imaged every 5 min from stage 10.5 onwards for 3 h with a Leica DMIRE2 computer-controlled Microscope (Leica, Bensheim, Germany) using the automator function of Open Lab imaging software (Improvision, Coventry, UK). In all cases, an area of the VAZ (Shih and Keller, 1992), slightly lateral of the dorsal midline was selected. For time-lapse studies from stage 12 onwards cell movements in the posterior paraxial mesoderm lateral to the notochord were followed. Migration paths and speed were analysed as described by Marlow *et al* (2002).

Immunocytochemistry

Explants were fixed in 4% formaldehyde buffered in 100 mM MOPS pH 7.4, 2 mM EGTA, and 1 mM $MgSO_4$ for 1 h at room temperature, transferred to Dent's fixative and stored at −20°C. After rehydration, explants were blocked in 20% horse serum, 1% blocking reagent (Roche Molecular Biochemicals, Mannheim, Germany) in TBST (50 mM Tris–HCl pH 7.5, 150 mM NaCl, 0.1% Tween 20). Incubation with the primary antibodies anti-phospho-H3 (Upstate, Lake Placid, NY), 12/101 (DSHB, Iowa), tor 70 (a generous gift of R Harland), and anti-β1-integrin (8C8, a generous gift of P Hausen) overnight at 4°C was followed by anti-rabbit Cy3, anti-mouse IgG-Cy3, or anti-mouse IgM-Cy2 (Dianova, Hamburg, Germany) for 4 h at room temperature. The explants were examined on a fluorescence microscope or a confocal laser scanning microscope (Leica, Bensheim, Germany). Phospho-H3-positive mitotic cells were counted exclusively in the mesodermal part of each explant in three randomly selected, independent areas of 166 μm^2 each.

SDS–PAGE and Western blotting

Whole embryos were lysed in NOP buffer (10 mM HEPES pH 7.4,150. mM NaCl, 2 mM EDTA, 1% NP-40) supplemented with complete® protease inhibitor (Roche Molecular Biochemicals, Mannheim, Germany). JNK was pulled down with anti-FL JNK (Santa Cruz Biotechnology, Santa Cruz, CA). Pull-downs of GTP-state small GTPases were carried out as described (Stahle *et al*, 2003) using 50 embryos per assay. For Western blotting procedures, proteins were transferred to PVDF membranes and incubated with the primary antibody (anti-FL JNK, anti-pJNK, anti-Rho A (Santa Cruz Biotechnology, Santa Cruz, CA); anti-GFP (Roche Molecular Biochemical, Mannheim, Germany); anti-Rac 1, anti-cdc 42 (BD Bioscience, Heidelberg, Germany)), followed by incubation with alkaline phosphatase-labelled goat anti-mouse IgG or goat anti-

rabbit IgG (Dianova, Hamburg, Germany) and developed using NBT/BCIP.

Supplementary data
Supplementary data are available at *The EMBO Journal* Online.

Acknowledgements

We thank R Rupp, M Kühl, E Nishida, R Harland, and H Steinbeisser for providing plasmids and reagents. We further thank H Steinbeisser and KM Kürner for sharing unpublished data and C Winter and M Welzel for technical support. This work was financed by the German Research Foundation grant We 1208.

References

Agius E, Oelgeschlager M, Wessely O, Kemp C, De Robertis EM (2000) Endodermal Nodal-related signals and mesoderm induction in *Xenopus*. *Development* **127:** 1173–1183

Axelrod JD, Miller JR, Shulman JM, Moon RT, Perrimon N (1998) Differential recruitment of Dishevelled provides signaling specificity in the planar cell polarity and Wingless signaling pathways. *Genes Dev* **12:** 2610–2622

Bastock R, Strutt H, Strutt D (2003) Strabismus is asymmetrically localised and binds to Prickle and Dishevelled during *Drosophila* planar polarity patterning. *Development* **130:** 3007–3014

Choi SC, Han JK (2002) *Xenopus* Cdc42 regulates convergent extension movements during gastrulation through Wnt/$Ca2^+$ signaling pathway. *Dev Biol* **244:** 342–357

Darken RS, Scola AM, Rakeman AS, Das G, Mlodzik M, Wilson PA (2002) The planar polarity gene strabismus regulates convergent extension movements in *Xenopus*. *EMBO J* **21:** 976–985

Davidson LA, Hoffstrom BG, Keller R, DeSimone DW (2002) Mesendoderm extension and mantle closure in *Xenopus laevis* gastrulation: combined roles for integrin alpha(5)beta(1), fibronectin, and tissue geometry. *Dev Biol* **242:** 109–129

Geis K, Aberle H, Kuhl M, Kemler R, Wedlich D (1998) Expression of the Armadillo family member p120cas1B in *Xenopus* embryos affects head differentiation but not axis formation. *Dev Genes Evol* **207:** 471–481

Habas R, Dawid IB, He X (2003) Coactivation of Rac and Rho by Wnt/Frizzled signaling is required for vertebrate gastrulation. *Genes Dev* **17:** 295–309

Heisenberg CP, Tada M, Rauch GJ, Saúde L, Concha ML, Geisler R, Stemple DL, Smith JC, Wilson SW (2000) Silberblick/Wnt11 mediates convergent extension movements during zebrafish gastrulation. *Nature* **405:** 76–81

Hollemann T, Panitz F, Pieler T (1999) *In situ* hybridization techniques with *Xenopus* embryos. In *A Comparative Methods Approach to the Study of Oocytes and Embryos*, Richter JD (ed) pp 279–290. Oxford: Oxford University Press

Huang C, Rajfur Z, Borchers C, Schaller MD, Jacobson K (2003) JNK phosphorylates paxillin and regulates cell migration. *Nature* **424:** 219–223

Hukriede NA, Tsang TE, Habas R, Khoo PL, Steiner K, Weeks DL, Tam PP, Dawid IB (2003) Conserved requirement of Lim1 function for cell movements during gastrulation. *Dev Cell* **4:** 83–94

Kaibuchi K, Kuroda S, Amano M (1999) Regulation of the cytoskeleton and cell adhesion by the Rho family GTPases in mammalian cells. *Ann Rev Biochem* **68:** 459–486

Keller R (2002) Shaping the vertebrate body plan by polarized embryonic cell movements. *Science* **298:** 1950–1954

Keller R, Davidson L, Edlund A, Elul T, Ezin M, Shook D, Skoglund P (2000) Mechanisms of convergence and extension by cell intercalation. *Philos Trans R Soc Lond B* **355:** 897–922

Keller R, Shih J, Domingo C (1992) The patterning and functioning of protrusive activity during convergence and extension of the *Xenopus* organiser. *Development Suppl 'Gastrulation'*, Stern CD, Ingham PW (eds) pp 81–91. Cambridge: Company of Biologists

Kilian B, Mansukoski H, Barbosa FC, Ulrich F, Tada M, Heisenberg CP (2003) The role of Ppt/Wnt5 in regulating cell shape and movement during zebrafish gastrulation. *Mech Dev* **120:** 467–476

Kim SH, Yamamoto A, Bouwmeester T, Agius E, De Robertis EM (1998) The role of paraxial protocadherin in selective adhesion and cell movements of the mesoderm during *Xenopus* gastrulation. *Development* **125:** 4681–4690

Kuehl M, Finnemann S, Binder O, Wedlich D (1996) Dominant negative expression of a cytoplasmically deleted mutant of XB/U-cadherin disturbs mesoderm migration during gastrulation in *Xenopus laevis*. *Mech Dev* **54:** 71–82

Kuehl M, Geis K, Sheldahl LC, Pukrop T, Moon RT, Wedlich D (2001) Antagonistic regulation of convergent extension movements in *Xenopus* by Wnt/β-catenin and Wnt/Ca^{2+} signaling. *Mech Dev* **106:** 61–76

Latinkic BV, Mercurio S, Bennett B, Hirst EM, Xu Q, Lau LF, Mohun TJ, Smith JC (2003) Xenopus Cyr61 regulates gastrulation movements and modulates Wnt signalling. *Development* **130:** 2429–2441

Marlow F, Topczewski J, Sepich D, Solnica-Krezel L (2002) Zebrafish rho kinase 2 acts downstream of wnt11 to mediate cell polarity and effective convergence and extension movements. *Curr Biol* **12:** 876–884

Marsden M, DeSimone DW (2001) Regulation of cell polarity, radial intercalation and epiboly in *Xenopus*: novel roles for integrin and fibronectin. *Development* **128:** 3635–3647

Marsden M, DeSimone DW (2003) Integrin–ECM interactions regulate cadherin-dependent cell adhesion and are required for convergent extension in *Xenopus*. *Curr Biol* **13:** 1182–1191

Miller JR, Rowning BA, Larabell CA, Yang-Snyder JA, Bates RL, Moon RT (1999) Establishment of the dorsal-ventral axis in *Xenopus* embryos coincides with the dorsal enrichment of dishevelled that is dependent on cortical rotation. *J Cell Biol* **146:** 427–437

Nieuwkoop PD, Faber J (1975) *Normal Table of Xenopus laevis (Daudin)*. Amsterdam: North Holland

Nishitoh H, Saitoh M, Mochida Y, Takeda K, Nakano H, Rothe M, Miyazono K, Ichijo H (1998) ASK1 is essential for JNK/SAPK activation by TRAF2. *Mol Cell* **2:** 389–395

Park M, Moon RT (2002) The planar cell-polarity gene stbm regulates cell behaviour and cell fate in vertebrate embryos. *Nat Cell Biol* **4:** 20–25

Penzo-Mendez A, Umbhauer M, Djiane A, Boucaut JC, Riou JF (2003) Activation of Gbetagamma signaling downstream of Wnt-11/Xfz7 regulates Cdc42 activity during *Xenopus* gastrulation. *Dev Biol* **257:** 302–314

Rawls AS, Wolff T (2003) Strabismus requires Flamingo and Prickle function to regulate tissue polarity in the *Drosophila* eye. *Development* **130:** 1877–1887

Sheldahl LC, Slusarski DC, Pandur P, Miller JR, Kuhl M, Moon RT (2003) Dishevelled activates Ca2+ flux, PKC, and CamKII in vertebrate embryos. *J Cell Biol* **161:** 769–777

Shih J, Keller R (1992) Patterns of cell motility in the organizer and dorsal mesoderm of *Xenopus laevis*. *Development* **116:** 915–930

Stahle M, Veit C, Bachfischer U, Schierling K, Skripczynski B, Hall A, Gierschik P, Giehl K (2003) Mechanisms in LPA-induced tumor cell migration: critical role of phosphorylated ERK. *J Cell Sci* **116:** 3835–3846

Tahinci E, Symes K (2003) Distinct functions of Rho and Rac are required for convergent extension during *Xenopus* gastrulation. *Dev Biol* **259:** 318–335

Takeuchi M, Nakabayashi J, Sakaguchi T, Yamamoto TS, Takahashi H, Takeda H, Ueno N (2003) The prickle-related gene in vertebrates is essential for gastrulation cell movements. *Curr Biol* **13:** 674–679

Topczewski J, Sepich DS, Myers DC, Walker C, Amores A, Lele Z, Hammerschmidt M, Postlethwait J, Solnica-Krezel L (2001) The zebrafish glypican knypek controls cell polarity during gastrulation movements of convergent extension. *Dev Cell* **1:** 251–264

Tree DR, Shulman JM, Rousset R, Scott MP, Gubb D, Axelrod JD (2002) Prickle mediates feedback amplification to generate asymmetric planar cell polarity signaling. *Cell* **109:** 371–381

Veeman MT, Slusarski DC, Kaykas A, Louie SH, Moon RT (2003) Zebrafish prickle, a modulator of noncanonical wnt/fz signaling, regulates gastrulation movements. *Curr Biol* **13:** 680–685

Wallingford JB, Harland RM (2002) Neural tube closure requires Dishevelled-dependent convergent extension of the midline. *Development* **129:** 5815–5825

Wessely D, Kim J, Geissert D, Tran U, De Robertis EM (2004) Analysis of Spemann organizer formation in *Xenopus* embryos by cDNA macroarrays. *Dev Biol* **269:** 552–566

Wharton Jr KA (2003) Runnin' with the Dvl: proteins that associate with Dsh/Dvl and their significance to Wnt signal transduction. *Dev Biol* **253:** 1–17

Wilson PA, Oster G, Keller R (1989) Cell rearrangement and segmentation in *Xenopus*: direct observation of cultured explants. *Development* **105:** 155–166

Winklbauer R, Medina A, Swain RK, Steinbeisser H (2001) Frizzled-7 signalling controls tissue separation during *Xenopus* gastrulation. *Nature* **413:** 856–860

Yamamoto A, Kemp C, Bachiller D, Geissert D, De Robertis EM (2000) Mouse paraxial protocadherin is expressed in trunk mesoderm and is not essential for mouse development. *Genesis* **27:** 49–57

Yamanaka H, Moriguchi T, Masuyama N, Kusakabe M, Hanafusa H, Takada R, Takada S, Nishida E (2002) JNK functions in the non-canonical Wnt pathway to regulate convergent extension movements in vertebrates. *EMBO Rep* **3:** 69–75

Zhong Y, Brieher WM, Gumbiner BM (1999) Analysis of C-cadherin regulation during tissue morphogenesis with an activating antibody. *J Cell Biol* **144:** 351–359